

Assessment of Extracellular Volume  
Fraction Using Dual-energy CT in  
Doxorubicin-induced Dilated  
Cardiomyopathy in a Rabbit Model:  
Comparison with Contrast-enhanced  
Magnetic Resonance Imaging and  
Histology

Yoo Jin Hong

Department of Medicine

The Graduate School, Yonsei University

Assessment of Extracellular Volume  
Fraction Using Dual-energy CT in  
Doxorubicin-induced Dilated  
Cardiomyopathy in a Rabbit Model:  
Comparison with Contrast-enhanced  
Magnetic Resonance Imaging and  
Histology

Directed by Professor Byoung Wook Choi

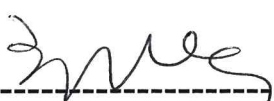
Doctoral Dissertation

Submitted to the Department of Medicine,  
the Graduate School of Yonsei University  
in partial fulfillment of the requirements for the degree  
of Doctor of Philosophy

Yoo Jin Hong

December 2014

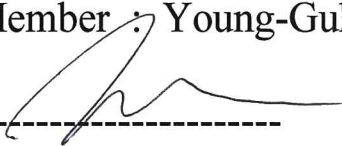
This certifies that the Doctoral Dissertation of  
Yoo Jin Hong is approved.

  
-----  
Thesis Supervisor : Byoung Wook Choi

  
-----  
Thesis Committee Member: Yeon Hyeon Choe

  
-----  
Thesis Committee Member: Hye-Yeon Lee

  
-----  
Thesis Committee Member : Young-Guk Ko

  
-----  
Thesis Committee Member : Jin Hur

The Graduate School  
Yonsei University

December 2014

### <Acknowledgements>

This work flourished due to the support and assistance of the following people. First, of all, I am extremely grateful to Dr. Byoung Wook Choi, Dr. Jin Hur, Dr. Hye-Jeong Lee, and Dr. Young Jin Kim for their teaching and guidance, and Yonsei University for providing resources to research this project, and Dongkook Pharmacy for financial support. I would also like to thank veterinarians Tai Kyung Kim (Konkuk University), Kyu Ri Park (Severance Hospital) for spending countless hours to develop animal models. Additionally, I wish to thank my brother Dong Hyun Hong (Erwin L. Hahn Institute, Essen, Germany) for his effort developing software and advising for this study. I also appreciate Jae Won Choi (CT Clinical Scientist, Siemens Healthcare, Seoul), Mun Young Paek (MR Clinical Scientist, Siemens Healthcare, Seoul), veterinarian Sae Jong Yoo (Konkuk University) for their tremendous time and effort for our experiments on every Tuesday late into the night. Thanks to Mary Ellen Wickum for her English proofreading and editing. Finally, I want to express deep gratitude to my family and husband Dr. Chul Hwan Park.

## <Table of Contents>

ABSTRACT .....	1
I. INTRODUCTION .....	3
II. MATERIALS AND METHODS .....	5
1. Animal model and drug administration .....	5
2. Animal preparation before CT and MR examinations .....	5
3. Animal inclusion and a flow chart of experiment .....	6
4. CT protocol .....	7
5. Dual-energy CT data post processing .....	8
6. MRI protocol .....	9
7. Image analysis .....	10
A. CT image analysis .....	10
(A) CT image analysis for the measurment of CT ECV (%) .....	10
(B) CT ECV map software development .....	11
(C) Evaluation of the image quality of CT iodine map .....	12
B. MR image analysis .....	14
(A) Functional analysis .....	14
(B) MR image analysis for the measurement of MR ECV fraction (%) ..	14
8. Histologic analysis .....	15
A. Collagen volume fraction (CVF,%) analysis .....	15
9. Statistical analysis .....	16

III.RESULTS .....	17
1. Physiological and functional data .....	17
2. Histological data .....	19
3. CT and MRI data .....	21
A. Validation of CT protocol and evaluation of image quality .....	21
B. CT and MR ECV .....	23
C. Comparison between CT, MR ECV and histologic collagen volume fraction .....	25
IV. DISCUSSION .....	26
V. CONCLUSION .....	29
REFERENCES .....	30
ABSTRACT (IN KOREAN) .....	34

## <List of Figures>

Figure 1. Flow chart of experiment .....	7
Figure 2. Measurement on CT and MR .....	11
Figure 3. The four scales of image quality of the iodine maps ..	13
Figure 4. The change of morphology and systolic function of left ventricle 16weeks after modeling .....	18
Figure 5. Mean histological collagen volume fraction (%) in control and group I-III .....	20
Figure 6. The histological example of control, group I-III .....	20
Figure 7. The change of CT ECV over time after contrast injection ·	21
Figure 8. Comparison of CT and MR ECV between control and group I-III .....	23
Figure 9. Bland-Altman Comparison of CT ECV and MR ECV ··	24

## <List of Tables>

Table 1. Physiological and functional data in all groups .....	17
Table 2. CT and MR extracellular volume (ECV) and histologic collagen volume fraction (CVF) in all groups .....	24



<ABSTRACT>

**Assessment of Extracellular Volume Fraction Using Dual-energy CT in  
Doxorubicin-induced Dilated Cardiomyopathy in a Rabbit Model:  
Comparison with Contrast-enhanced Magnetic Resonance Imaging and  
Histology**

Yoo Jin Hong

*Department of Medicine  
The Graduate School, Yonsei University*

Directed by Professor Byoung Wook Choi

**Purpose:**

To assess the feasibility of extracellular volume (ECV) fraction using dual-energy computed tomography (CT) and to compare it with magnetic resonance imaging (MRI) T1 mapping and histologic findings.

**Materials and methods:**

A dilated cardiomyopathy rabbit (DCR) model was made by injecting doxorubicin into the rabbits (adult male New Zealand white rabbits, 3-4 kg) at doses of 1.0 mg/kg twice a week. Every rabbit underwent both dual-energy CT and magnetic resonance imaging (MRI) within two hours with pre-/post-contrast T1 mapping using modified Look-Locker inversion recovery (MOLLI) sequence, late gadolinium enhancement (LGE), and cine MR on a clinical 3-T system. The rabbits underwent CT and MR examination before drug administration (control group) and DCR model at various post-modeling intervals (6 weeks, 12 weeks or 16 weeks after DCR modeling). CT ECV was quantitatively assessed by measuring Hounsfield units (HUs) in the septum in a cardiac

short-axis view on iodine maps. MR ECV was assessed in the same area with CT. The left ventricle ejection fraction (LVEF) was obtained from the cine MR images using Simpson's method.

### **Results:**

Fifteen rabbits were scanned prior to modeling, and then four controls were sacrificed for histology. The remaining eleven underwent DCR modeling and were scanned at various post-modeling intervals (Group I; 6-week modeling,  $n = 11$ ; group II; 12-week modeling,  $n = 8$ ; and group III; 16-week modeling,  $n = 5$ ). The mean CT ECV values (%) of group I-III were significantly higher than control group (Control vs. group I vs. group II vs. group III; 28.5 (range, 25.9-31.3) vs. 35.3 (range, 30.2-40.1) vs. 41.9 (range, 35.6-44.1), vs. 42.1 (range, 39.2-46.4),  $p < 0.001$ ) and there was a good correlation between CT ECV and MR ECV ( $r = 0.888$ ,  $p < 0.001$ ) and between CT ECV and degree of fibrosis ( $r = 0.811$   $p < 0.001$ )

### **Conclusion:**

ECV using dual-energy CT shows good correlation with MRI and histology. Noninvasive measurement of ECV in animals with doxorubicin-induced diffuse myocardial fibrosis is feasible with dual-energy CT without misregistration errors.

---

Key words: magnetic resonance imaging, endomyocardial fibrosis, extracellular space, extracellular matrix, radiography, dual-Energy scanned projection, multidetector computed tomography

**Assessment of Extracellular Volume Fraction Using Dual-energy CT in  
Doxorubicin-induced Dilated Cardiomyopathy in a Rabbit Model:  
Comparison with Contrast-Enhanced Magnetic Resonance Imaging and  
Histology**

Yoo Jin Hong

*Department of Medicine  
The Graduate School, Yonsei University*

Directed by Professor Byoung Wook Choi

**I. INTRODUCTION**

Diffuse myocardial fibrosis is a final common end point in the pathological process of myocardial disease.<sup>1,2</sup> Diffuse myocardial fibrosis indicates irreversible damage to the myocardium. This insult to the myocardial structure is known to be associated with adverse cardiac events: heart failure, hospitalization, sudden death, etc. in various types of cardiomyopathy.<sup>3-5</sup>

Myocardial T1 mapping is an emerging technique that could improve detection of diffuse interstitial myocardial fibrosis using measurements of extracellular volume (ECV) fraction. ECV fraction can be used to quantitatively evaluate myocardial fibrosis and, subtle myocardial change in various cardiac diseases.<sup>1,6-9</sup> ECV fraction has been demonstrated yielding a good correlation with histologic finding.<sup>10</sup> A few recent studies reported that computed tomography (CT) utilizing iodine contrast was useful to detect diffuse myocardial fibrosis.<sup>11-13</sup> Nacif et al. demonstrate in clinical practice the application of the theory of ECV fraction using iodine contrast agent in diffuse fibrosis patients based on the theory that iodine contrast

agents are also extracellular tracers having the same distribution area as gadolinium contrast agents.<sup>12-15</sup> They used conventional CT with pre- and post-contrast CT scans. The ECV measured on CT scan correlated well with that of MRI.<sup>12,13</sup>

In a study of in vivo models by Gerber et al., contrast-enhanced CT characterized acute and chronic myocardial infarction with contrast patterns similar to contrast-enhanced magnetic resonance imaging (MRI). Their study demonstrated similar contrast kinetics and distribution pattern between an iodine and a gadolinium contrast agent in infarcted and noninfarcted myocardium.<sup>15</sup> Gerber et al. suggested this may be due to these iodine and gadolinium tracers' similar molecular weights and extracellular volume of distribution even though the tracers' molecular structures were different.<sup>14,15</sup> Due to the kinetic similarities between gadolinium agents used in MRI and iodine contrast agents used in CT there can be similar imaging applications.

The general advantages of CT in comparison with MRI are faster, widely available, and cheaper imaging.<sup>11</sup> The specific advantages of CT in the evaluation of the heart are the possibility of simultaneous evaluation of coronary arteries as well as the evaluation of whole myocardium. However, there are no prior reports on the quantification of the ECV using dual-energy CT in diffuse myocardial fibrosis patients. Dual-energy CT is an advanced imaging technique that can provide material composition information by using two data sets of different X-ray spectra.<sup>16</sup> The major advantages of dual-energy CT over conventional CT in this study are to differentiate iodine component on delayed contrast-enhanced imaging without misregistration artifact.

We hypothesized that dual-energy CT would be valuable for extracting the iodine component of the myocardium and assessing CT ECV. The purposes of this study were to validate ECV using dual-energy CT and to compare it with that of contrast-enhanced MRI and to access

histologic collagen volume fraction (CVF) in dilated cardiomyopathy rabbit models.

## **II. MATERIALS AND METHODS**

### **1. Animal model and drug administration**

Twenty adult male New Zealand white rabbits weighing between 3-4 kg were included in this study. Among them, four rabbits were not subjected to drug administration for the evaluation of histology as a control group. In the other rabbits, doxorubicin (Doxorubicin hydrochloride, Cayman Chemical, Ann Arbor, MI) was injected at doses of 1.0 mg/kg twice a week until they were sacrificed for histologic evaluation. The ear was clipped, the skin was sterilized, and the auricular vein was accessed by the introduction of a 21-gauge needle. The doxorubicin (1.0 mg/kg) was diluted with 20 ml 0.9% sterile saline. The diluted drug was slowly injected for 3 minutes with bolus injection method. Antibiotics sulfamethoxypyridazine and trimethoprim (Amphoprim bolus; Virbac, New Zealand) were administered every day from 5 weeks after the DCR modeling began. Hematocrit (Hct) levels were measured immediately before the CT examinations.

### **2. Animal preparation before CT and MR examinations**

The rabbits underwent CT and MR examination before drug administration (control group) and dilated cardiomyopathy rabbit (DCR) models at the end of post-modeling intervals (6 weeks, 12 weeks or 16 weeks after DCR modeling). Before CT examination the rabbits were anaesthetized with an intra-muscular injection of tiletamine (30mg/kg, Zoletil; Vibac Laboratories, Carros, France) and xylazine (5mg/kg, Rompun; Bayer, Korea), and the rabbits were shaved on the anterior chest wall for electrocardiographic (ECG) electrodes. Two venous accesses were prepared

at both auricular veins. The first venous access was used for contrast injection, and the second venous access was used for medetomidine hydrochloride (0.3mg/kg, Tomidine®; Provet veterinary products Ltd. Istanbul, Turkey) administration. Venous sampling was done for Hct values of all rabbits. After anesthesia, the animals were intubated, and mechanically ventilated using a mechanical ventilator (Mekant, MEKICS, Seoul, Korea) with a mixture of oxygen and isoflurane for CT and MR scanning. The ventilator was not MRI-compatible, so, it was located outside the MRI room with its long respiratory tubes entering the room through a hole in the wall.

### **3. Animal inclusion and a flow chart of experiment**

Twenty rabbits were included. Among them, four control rabbits were sacrificed after CT and MRI scanning for the histologic evaluation as a control group. The other sixteen rabbits were subjected to drug administration for DCR modeling. Five rabbits died during the modeling periods due to severe anemia (n = 3) or infection (pneumonia, n = 2). At the end of the 6-week modeling period, Group I (n = 11) underwent post-modeling CT and MRI scans. Afterwards 3 rabbits were sacrificed for the histologic evaluation at the 6-week modeling period. The other eight rabbits (Group II; n = 8) continued DCR modeling, and underwent post-modeling CT and MRI scans at the end of the 12-week modeling period. Next 3 rabbits were sacrificed for the histologic evaluation at the 12-week modeling period. The other five rabbits continued DCR modeling (Group III; n = 5), and underwent post-modeling CT and MRI scans at the end of the 16-week modeling period. After post-modeling CT and MRI scanning, the five remaining rabbits were sacrificed for a histologic evaluation at the 16-week modeling period (Fig 1).

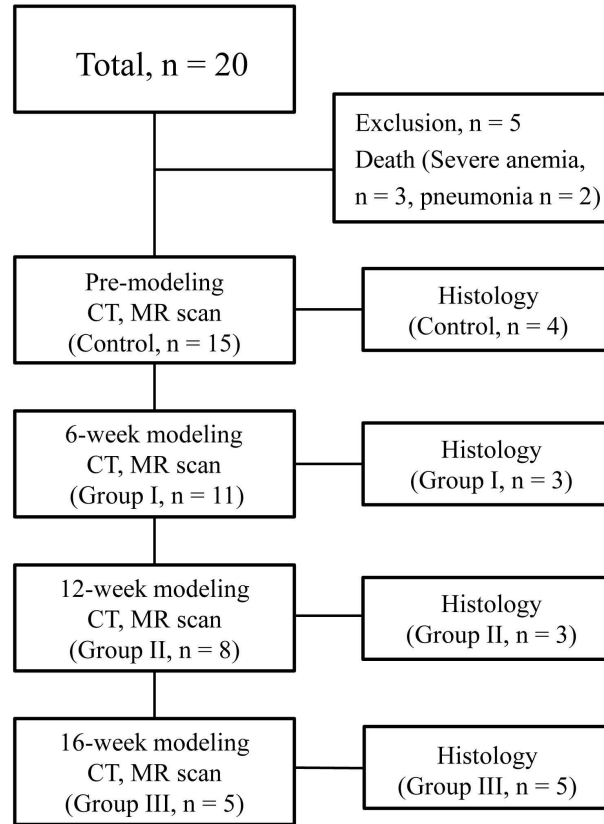


**Figure 1.** Flow chart of experiment

#### 4. CT protocol

Dual-energy CT was performed using a dual-source CT (Somatom Definition Flash, Siemens Healthcare, Forchheim, Germany) with retrospectively ECG-gated helical scanning without ECG pulsing. Scan parameters were as follows: 185 effective mAs at 100kV, and 157 effective mAs at 140 kV with a tin filter,  $64 \times 0.6$  mm collimation, 0.32 pitch factor, and 0.28 second rotation time. Images were acquired from the apex of the heart to the costophrenic angles in the caudocranial direction. After bolus injection of 2 ml/kg contrast medium (Pamiray 370, Dongkook

Pharmaceutical, Seoul, Korea) followed by 8-10 mL of normal saline at 1.5-1.7 mL/s through the auricular vein of rabbits. The first post-contrast scan started at 3 minutes, and additional scans were done at 5, 7, 9, 11, 13 and 20 minutes after the attenuation value reached 100 Hounsfield units (HUs) in the thoracic aorta using the bolus tracking technique. Each rabbit was given a bolus injection of 0.3 mg/kg of medetomidine to reduce heart rate 30 seconds before each scanning.

## **5. Dual-energy CT data post processing**

CT data sets were assessed by two radiologists (Y.J.H., C.H.P.) with more than nine years of experience in cardiac CT. All scans were processed and read on a dedicated workstation equipped with dual-energy post processing software (Syngo MMWP VE 36A, Siemens Medical Solutions, Forchheim, Germany). The weighted average image was approximately 120 kV and was automatically generated from a combination of the 140 kV and 100 kV data. Dual-energy post processing was performed with the heart perfusion application (Siemens dual-energy software). First an image-based analysis was run with the low-energy and high-energy images. Next iodine maps were created based on a three-material decomposition of soft tissue, air, and iodine. This showed the distribution of iodine in the whole left ventricle (LV) myocardium. Color-coded iodine maps were also made then merged with corresponding CT images. Soft-tissue settings were used to create fusion images. This allowed simultaneous depiction of myocardium and myocardial delayed contrast-enhancement. All images were reconstructed on short axis plane. For image analysis, reconstructed iodine maps and merged color-coded iodine maps were transferred to a picture archiving and communication system (PACS) (Centricity 1.0; GE Medical Systems, Mt Prospect, IL, USA).



## 6. MRI protocol

MRI was performed within 2 hours of dual-energy CT. MRI imaging was performed using a 3.0-T MR scanner (Magnetom Trio Tim, Siemens Healthcare, Erlangen, Germany) with a 6 channel anterior body matrix coil and 12 channel posterior head matrix coil. Localization of the heart was performed with steady state free precession sequence under ECG gating. Cine, late gadolinium enhancement (LGE), pre- and post-contrast T1 mapping images were acquired. For cardiac functional analysis, cine images were acquired using a TrueFISP sequence in a short-axis plane orientation using the following parameters: TR = 3.9 ms, TE = 1.68 ms, flip angle = 50°, 25 phases, slice thickness = 3 mm, slice gap = 0.6 mm, acquisition matrix = 160 × 160, and a field of view = 150 × 135mm<sup>2</sup>. T1 mapping was performed with a modified Look-Locker inversion recovery (MOLLI) sequence during the end expiratory period in a mid-ventricular short axis view-. For the MOLLI imaging, three nonselective inversion pulses; steady state free precession single-shot readout in mid-diastolic phase was employed using the following parameters: field of view = 150 × 121 mm, acquisition matrix = 192 × 155, slice thickness = 3.5 mm, TR = 3.6 ms, TE = 1.45 ms, minimum inversion time 105ms, inversion time increment 60 ms, flip angle = 35°, GRAPPA parallel acquisition factor = 2, four images are acquired after the first inversion pulse, followed by a pause of six heart beats, then four images are acquired after the second inversion pulse, followed by a pause of six heart beats, then six images are acquired after a third inversion pulse. Fully automated non-rigid motion correction was applied to register the individual TI images before inline T1fitting was performed using a mono-exponential 3-parameter fit. Pre-T1 mapping images were acquired before the injection of contrast. Post-contrast T1 mapping images were acquired 13 minutes after the injection of a 0.2 mmol/kg intravenous dose of gadolinium

contrast agent (Omniscan®; GE Healthcare, Princeton, NJ). LGE MR imaging was obtained 15min after the injection of the contrast agent using a magnitude- and phase-sensitive inversion recovery (PSIR) prepared steady state free precession sequence, with the inversion time adjusted to null the normal myocardium. LGE images were obtained along the same axis plane, and with the same slice thickness as used for the T1 mapping images (TR = 3.3 ms, TE = 1.41 ms, FOV =  $200 \times 162\text{mm}^2$ , thickness 3.5 mm, matrix =  $224 \times 201$ , non-selective inversion recovery, flip angle =  $70^\circ$ , BW 770 Hz/pixel, number of trigger pulses = 2). The appropriate inversion time prior to LGE MR imaging was determined using a steady state free precession sequence with varying inversion times from 150 to 650 ms to null the signal from the normal myocardium.

## **7. Image analysis**

Two radiologists (Y.J.H., C.H.P.) with nine years of experience in cardiovascular image interpretation analyzed all CT, MR images each other and interobserver agreement was assessed.

### **A. CT image analysis**

#### **(A) CT image analysis for the measurement of CT ECV (%)**

CT ECV (%) was measured on a PACS system. We chose one image at mid LV where papillary muscles were visible from the 13 minute iodine map images reconstructed on the short axis plane. The selected image was used for a regional analysis of LV myocardium. The regions of interest (ROI) were drawn at the septal segment as large as possible and round ROI larger than  $10\text{-}15\text{mm}^2$  was drawn in LV cavity avoiding papillary muscle (Fig. 2a). Mean attenuation in HU at ROI was recorded. Myocardial CT ECV ( $\text{ECV}_m$ ) was calculated by using the following formula.

$$ECV_m = (HU_m/HU_b) \times (1 - Hct),$$

where  $ECV_m$  = myocardial ECV in dual-energy CT,  $HU_m$  = HU of ROI of myocardium on the iodine map,  $HU_b$  = HU of blood pool on the iodine map, Hct = hematocrit value.

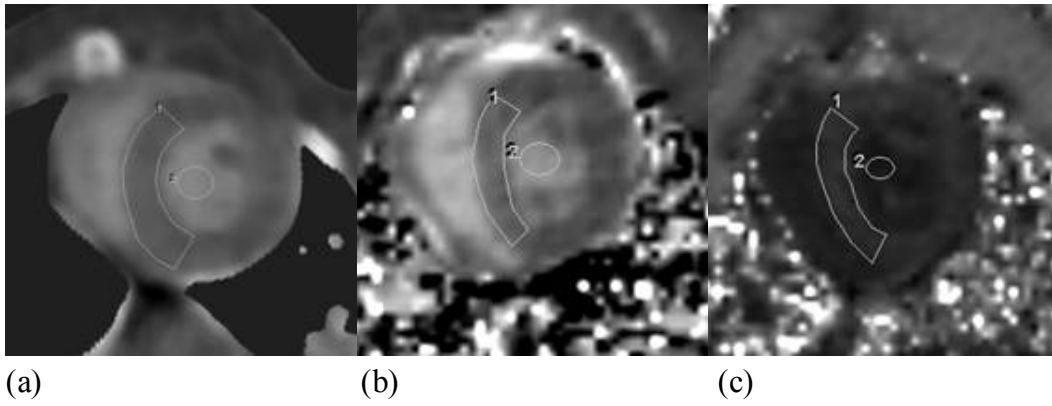


**Figure 2.** Measurement on CT and MRI: short axis cardiac images were used to define the region of interest (ROI) for fibrosis in the rabbit control and experimental groups.

- (a) The ROI on CT was drawn at the septal segment of the LV and LV cavity on the iodine map
- (b) The ROI on the pre-contrast MR image was drawn at the same septal segment of the LV and LV cavity as the CT.
- (c) The ROI on the post-contrast MR image was drawn at the same septal segment of the LV and LV cavity as the CT, and the pre-contrast MR image.

### **(B) CT ECV map software development**

In this study, CT ECV map were quantified by a custom-developed software package written in MATLAB (Version 2014a, The MathWorks, Inc., Natick, Massachusetts, United States). This software package is

semi-automated GUI (Graphical User Interface), and it takes less than 10 seconds using 2.3GHz Intel Core i7 computer with 8GB RAM running Mac OSX 10.9 for all processing steps. This software calculated ECV values based on the same equation mentioned above, and provided color-coded ECV maps of the whole myocardium. We exported iodine map images from PACS system with the DICOM (Digital Imaging and Communications in Medicine) file format. We reconstructed these DICOM images into one volume file (.vol extension), which contained all the slices. Then, we loaded this volume file on the software, and checked all the slices to find the blood pool area for ECV maps. We drew a blood pool ROI (region of interest) manually, and also input the hematocrit value required for ECV calculation. After this step, the software calculated ECV values and ECV maps of each slice, which were depicted on a color-coded map with a percentage scale. Additionally, we used each slice's ECV value to make an ECV profile table to illustrate the ECV changes between slices.

### **(C) Evaluation of the image quality of CT iodine map**

Image qualities of the iodine maps scanned at 3, 5, 7, 9, 11, 13 and 20 minutes after contrast injection were determined using subjective four-point scales (Fig 3). 4 = excellent, no image degradation, clear demarcation between left ventricle myocardium and cavity; 3 = good, minor degree of image degradation without affecting diagnostic accuracy; 2 = adequate, moderate degree of image degradation slightly affecting diagnostic accuracy, however, images were still used for diagnosis; 1 = poor, severe image degradation which greatly affected diagnostic accuracy, and resulted in non-diagnostic poor images.

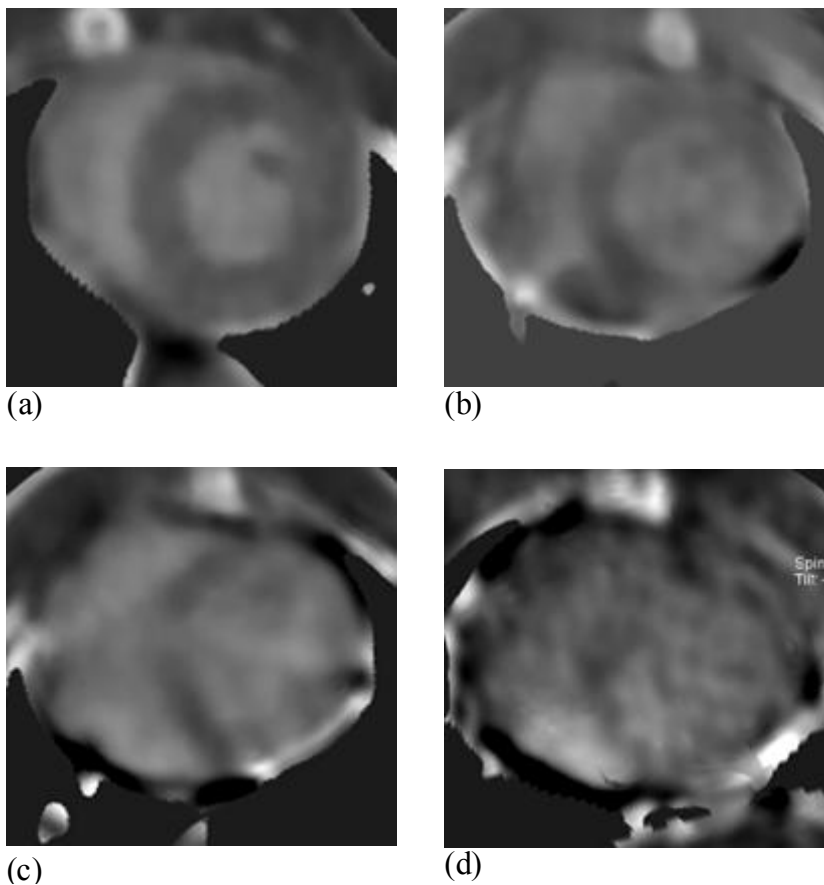


**Figure 3.** The four scales of image quality of the iodine maps

- (a) Image quality score 4; excellent, no image degradation, clear demarcation between left ventricle myocardium and cavity
- (b) Image quality score 3; good, minor degree of image degradation without affecting diagnostic accuracy
- (c) Image quality score 2; adequate, moderate degree of image degradation slightly affected diagnostic accuracy
- (d) Image quality score 1; poor, severe image degradation which greatly affected diagnostic accuracy

## **B. MR image analysis**

### **(A) Functional analysis**

All MR cine images were transferred to a commercially available software (Argus; Siemens Medical Solutions, Erlangen, Germany). The function of the LV was assessed using Simpson' method on short-axis cine MR images. The endocardial and epicardial borders of the LV wall were delineated semiautomatically on the end-diastolic and end-systolic images. The papillary muscles and trabeculations were excluded from LV myocardium. LV end-diastolic volume (LVEDV) and LV end-systolic volume (LVESV) were automatically measured. LV ejection fraction (LVEF, %) is calculated as follows:

$$\text{LVEF (\%)} = 100 \times (\text{LVEDV} - \text{LVESV}) / \text{LVEDV}^{17,18}$$

### **(B) MRI image analysis for the measurement of MR ECV fraction (%)**

All MR images were transferred to a PACS system for image analysis. To quantify MR ECV, short axis plane pre-and post-contrast T1 mapping images were needed. We selected one pre- and one post-contrast T1 mapping image at mid LV where papillary muscles were visible. On those images, the same septal segment measured on CT was selected and the region of interests (ROIs) were drawn. For a measurement of T1 value of blood, the round ROI larger than 10-15 mm<sup>2</sup> was drawn in LV cavity avoiding papillary muscles (Fig 2b-c). The ECV fraction of myocardium was calculated from the equation using Hct, pre-and post-contrast T1 values of myocardium and LV blood as follows.

$$\text{ECV} = [ (1/\text{T1}_{\text{post-contrastmyocardium}}) - (1/\text{T1}_{\text{pre-contrastmyocardium}}) ] / [ (1/\text{T1}_{\text{post-contrastblood}}) - (1/\text{T1}_{\text{pre-contrastblood}}) ] \times (1 - \text{Hct})$$

## **8. Histologic analysis**

For histologic analysis, samples from left ventricle were obtained immediately after euthanasia using KCl injection. And the heart was fixed in 10% paraformaldehyde buffered with phosphate. After 1 week of fixation, the tissue was dissected into short axis plane at mid LV level, where papillary muscles were visible, using rabbit heart slicer (Zivic instruments, Pittsburg, PA, USA). The fragments were dehydrated in solutions of decreasing concentration of alcohol, cleared in xylene and embedded in paraffin. Three micrometers section were obtained and stained with picrosirius red stain.

### **A. Collagen volume fraction (CVF,%) analysis**

An independent researcher performed the histopathologic analysis while blinded to the CT and MRI results. Each histopathologic section was obtained at the septal segment at mid LV. Next, the section was digitally photographed with high-power magnification ( $\times 200$ ) and transferred to the computer. The histopathological image analysis was performed with ImageJ (National Institute of Health, Bethesda, MD). First, the image was converted into 8 bit unsigned binary gray scale with tiff (Tagged Image File Format). Second, a histogram map was created for thresholding segmentation between fibrosis and myocardial cells. Normally, fibrosis is distributed on signal intensity scale of approximately 0 to 30 and myocardial cells are distributed on signal intensity scale of 200 to 255 on 8 bit binary image. Third, segmentation was optimized by manipulating two thresholds at the location of pixel intensity 40 and 180. Based on these two values, the pixel numbers in these two areas were counted, and estimated the fibrosis to myocardium ratio (in percentage) on the image. 3 images were assessed per model, and the mean percent fibrosis was obtained.

## 9. Statistical Analysis

All continuous data are expressed as means  $\pm$  standard deviations (SD) and categorical variables are presented as numbers or percentages. CT ECV, MR ECV at 13 minutes were compared with histologic CVF by Spearman correlation. The relationship between myocardial CT ECV and MR ECV at 13 minutes was also assessed by  $r$  using mixed model. We evaluated the change in CT ECV values according to the scan time, and the change in CT ECV and MR ECV according to modeling time (between control group, Group I-III) using a linear mixed model as implemented in the MIXED procedure of SAS (version 9.2; SAS Institute, Cary, NC, USA) with restricted maximum likelihood estimation. Agreement between these measures of CT, MR ECV between two observers was assessed by intraclass correlation coefficient (ICC). The Bland-Altman plot between CT ECV and MR ECV at 13 minutes was demonstrated.  $P$  value less than 0.05 was considered to indicate statistical significance. All statistical analyses were performed with the Statistical Package for the Social Science (SPSS) software (Version 20; SPSS Inc., Chicago, IL, USA), SAS (Version 9.2; SAS Institute Inc., Cary, NC, USA.) or MedCalc (Version 12.7.0; MedCalc Software, Ostend, Belgium)



### III. RESULTS

A total of fifteen control and eleven DCR models were included in this study. For the image analysis, CT, MR images of the 15 control models, 11 Group I (6-week DCR) rabbits and 8 Group II (12-week DCR), and 5 Group III (16-week DCR) rabbits were evaluated. For the histologic analysis, 4 control rabbits, 3 Group I (6-week DCR) rabbits and 3 Group II (12-week DCR), and 5 Group III (16-week DCR) rabbits were analyzed.

#### 1. Physiological and functional data

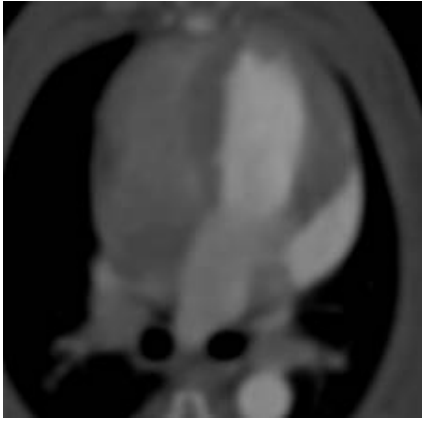
The hemoglobin level at 6 weeks was seen significantly decreased in the DCR models compared to the control group. The initial hemoglobin level of control group was 42.0% (range, 33-55) and 6 week hemoglobin level was 33.2% (range, 19-46) (Table 1) In DCR model, ventricular chamber enlargement and left ventricular wall thinning is noted (Fig 4). The mean LVEF of post -modeling group II, III were significantly lower than control groups (Table 1).

**Table 1.** Physiological and functional data in all groups

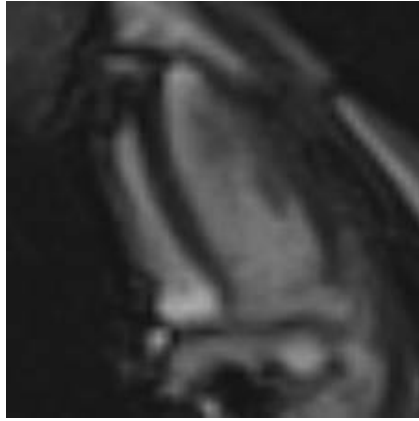
	Control (Pre-model, n = 15)	Group I (6 week DCR <sup>‡</sup> , n = 11)	Group II (12 week DCR, n = 8)	Group III (16 week DCR, n = 5)
Hemoglobin (%) <sup>*</sup>	42.0 (33.0-55.0)	33.2 (19.0-46.0)	33.2 (25.0-42.0)	36.1 (24.0-43.0)
Left ventricular ejection fraction (%) <sup>*</sup>	56.3 ± 6.4	41.6 ± 2.8	31.9 ± 15.3 <sup>†</sup>	36.7 ± 2.2 <sup>†</sup>
End diastolic volume (ml) <sup>*</sup>	2.25 ± 0.80	2.04 ± 0.70	2.32 ± 0.56	3.08 ± 0.86
End systolic volume (ml) <sup>*</sup>	1.00 ± 0.43	1.19 ± 0.41	1.64 ± 0.77	2.02 ± 0.63
Stroke volume (ml) <sup>*</sup>	1.24 ± 0.39	0.85 ± 0.29	0.69 ± 0.22	1.19 ± 0.46
Cardiac output (ml/min) <sup>*</sup>	0.20 ± 0.86	0.11 ± 0.05	0.08 ± 0.04	0.05 ± 0.10
Left ventricle mass (g) <sup>*</sup>	2.53 ± 0.60	2.65 ± 0.72	3.15 ± 0.75	3.52 ± 0.44

\* Mean ± SD, <sup>†</sup>  $p < 0.05$ , statistically significant

<sup>‡</sup> DCR = dilated cardiomyopathy rabbit model



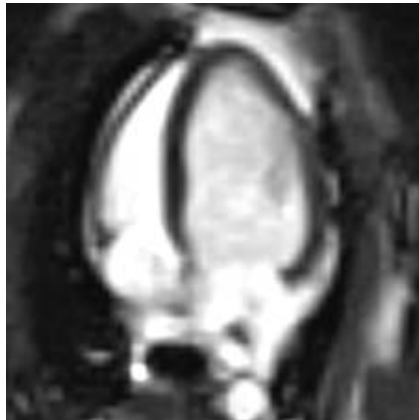
(a)



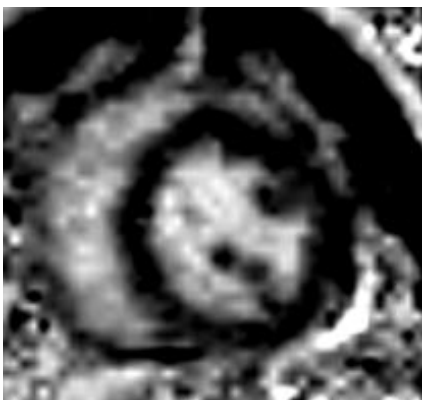
(b)



(c)



(d)



(e)

**Figure 4.** The comparison of CT axial, 4-chamber cine MR, and LGE MR image of left ventricle before and 16 weeks after modeling

(a-b) CT axial image (a), and 4-chamber cine MR image (b) of a control model, left ventricle ejection fraction = 53.5%

(c-e) CT axial image (c), and 4-chamber cine MR image (d), and the LGE MR image (e) of 16 week DCR model, left ventricle ejection fraction = 36.7%; Left ventricular systolic function decreased and left ventricular globular dilatation and wall thinning is noted. On the LGE MR image, there was no focal delayed enhancement on LV myocardium.

## **2. Histological data**

On picrosirius red stain, the area stained red represented collagen fibers located in the extracellular space. The collagen volume fraction (CVF) of a 6-week model showed a mild increase compared to the control model. The CVF increased again between the 6-week and 12-week models. There was a dramatic increase in the CVF between 12-week, and 16-week models (Fig 5).

The histological examples of control, group I-III demonstrate (a) 2.5%, (b) 5.0%, (c) 24.9%, and (d) 44.7% CVF (Fig 6). Mean CVF of control group (n = 4) was 2.6% (range, 2.0-3.3). That of group I (n = 3), group II (n = 3), group III (n = 5) were 10.6% (range, 4.7-21.9), 21.5% (range, 10.7-37.7), 48.3% (range, 24.6-67.2) (Fig 5). The difference between group III and group II was larger than that of group II and group I. The graph shows that fibrosis was more accelerated as time went.

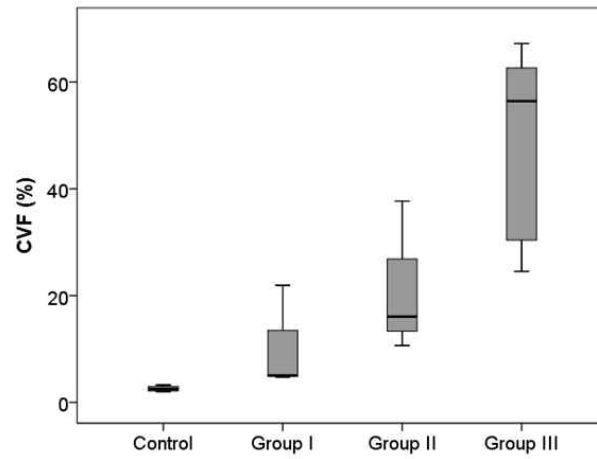


**Figure 5.** Mean histological collagen volume fraction (CVF,%) in control and group I-III

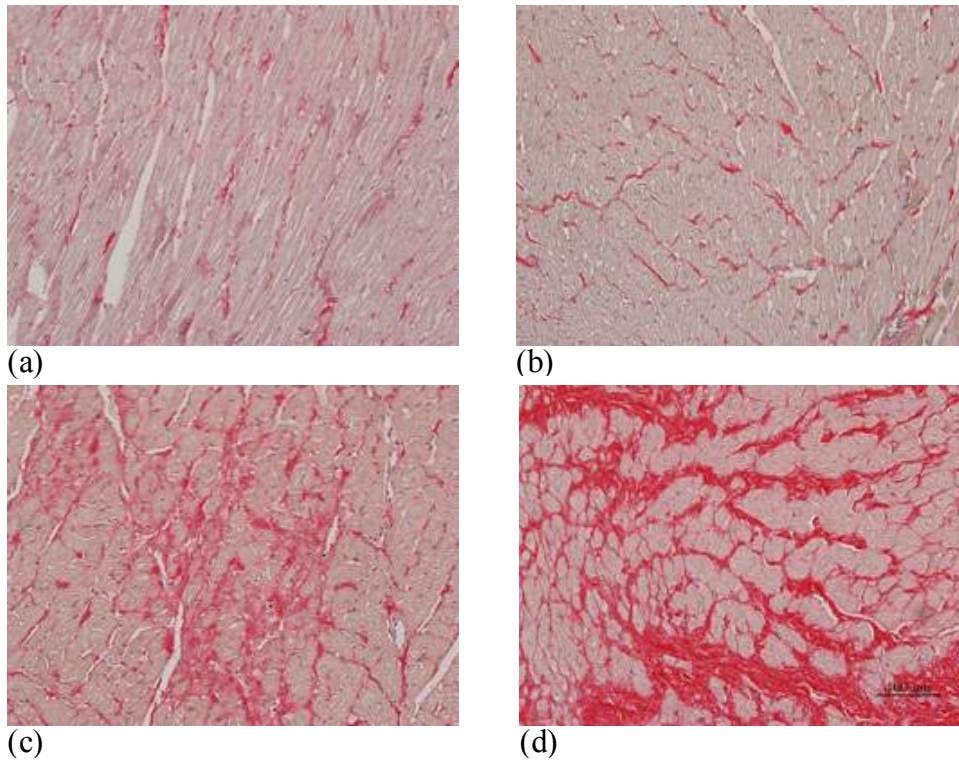


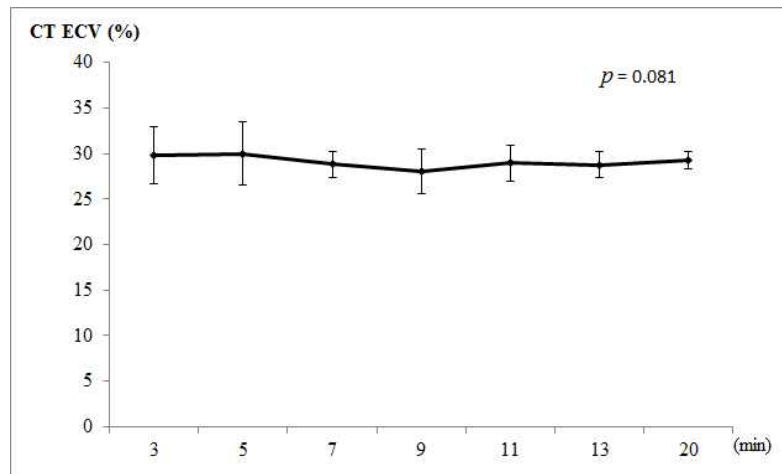
**Figure 6.** The histological example of control, group I-III

The histological example of control, group I-III demonstrate (a) 2.5%, (b) 5.0%, (c) 24.9%, and (d) 44.7% CVF, each other (picosirius red: original magnification  $\times 200$ .)

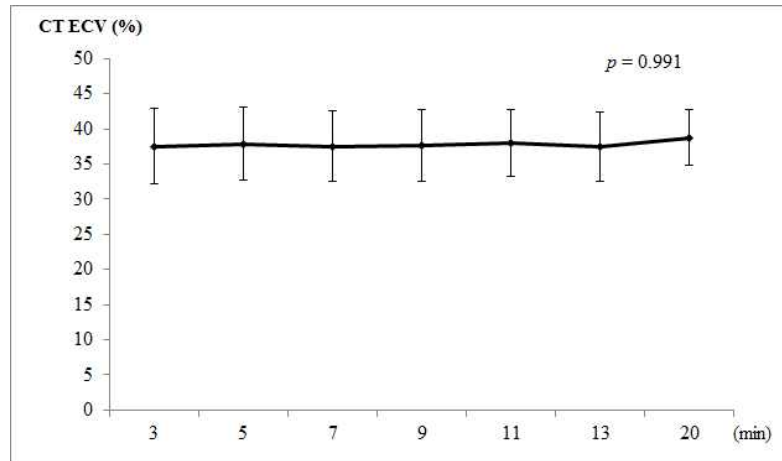
### 3. CT and MRI data

#### A. Validation of CT protocol and evaluation of image quality

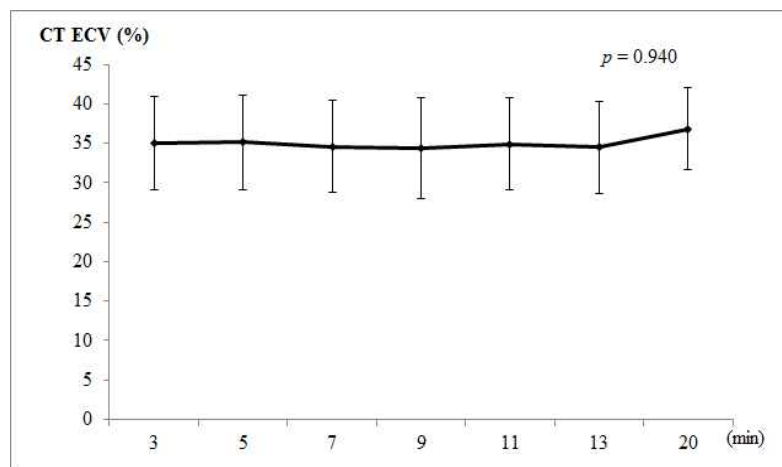
To determine the proper scanning and find the stabilized point of CT ECV, we scanned once then three minutes later, thereafter every two minutes until 20 minutes. CT showed no significant change from 3 minutes to 20 minutes in all groups (control group:  $p = 0.081$ , post-modeling group:  $p = 0.991$ , all groups:  $p = 0.940$ ) (Fig 7a-c). A total of 254 septal segments were analyzed in all groups. Of these, 238 (93.7%) segments were diagnostic (score = 2-4): excellent (score = 4) in 61 (24.0%) segments, good (score = 3) in 106 (41.7%) segments, adequate (score = 2) in 71 (28.0%) segments, and 16 (6.3%) segments were nondiagnostic (score = 1).



(a)



(b)



(c)

**Figure 7.** The change of CT ECV over time after contrast injection

- (a) The change of CT ECV over time after contrast injection in control group ( $p = 0.081$ )
- (b) The change of CT ECV over time after contrast injection in post-modeling groups (group I-III) ( $p = 0.991$ )
- (c) The change of CT ECV over time after contrast injection in all rabbits ( $p = 0.940$ )

## B. CT and MR ECV

The mean CT ECV of control group (n = 15) was 28.5% (range, 25.9-31.3). Those of group I-III were 35.3% (range, 30.2-40.1), 41.9% (range, 35.6-44.1), 42.1% (range, 39.2-46.4). The mean MR ECV of control group (n = 15) was 28.8% (range, 26.1-30.8). Those of group I-III were 32.6% (range, 29.9-34.3), 35.8% (range, 31.0-39.8), and 41.3% (range, 38.4-47.3) (Fig 8, Table 2). The interobserver agreement for CT, MR ECV measurements was good (ICC (95% CI), 0.902 (0.920-0.947) for CT ECV; ICC, 0.953 (0.911-0.975) for MR ECV). Bland-Altman plot between CT ECV and MR ECV at 13 minutes was demonstrated at Figure 9.

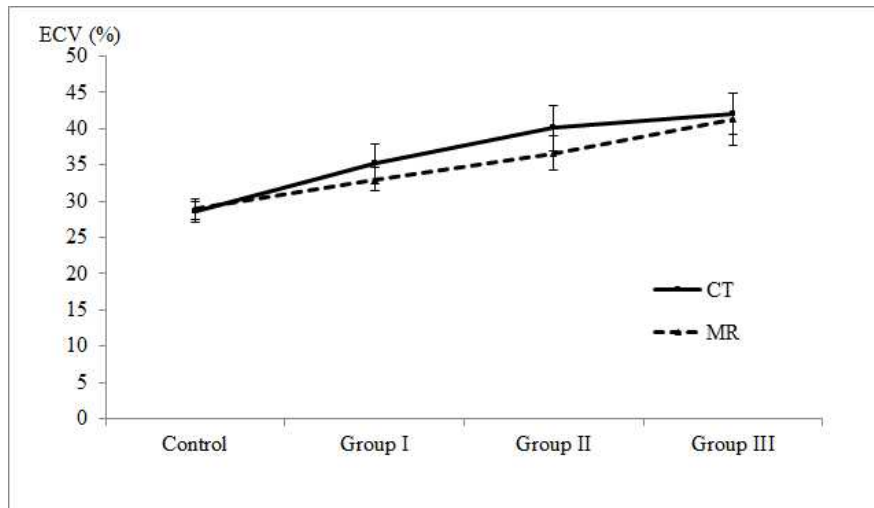


**Figure 8.** Comparison of CT and MR ECV between control and group I-III

**Table 2.** CT, MR extracellular volume (ECV) and histologic collagen volume fraction (CVF) in all groups

	Control (Pre model, n = 15)	Group I (6 week DCR †, n = 11)	Group II (12 week DCR, n = 8)	Group III (16 week DCR, n = 5)
CT ECV (%) *	28.5 (25.9-31.3)	35.3 (30.2-40.1)	41.9‡ (35.6-44.1)	42.1§ (39.2-46.4)
MR ECV (%) *	28.8 (26.1-30.8)	32.6 (29.9-34.3)	35.8‡ (31.0-39.8)	41.3§ (38.4-47.3)
CVF (%) *	2.6 <sup>  </sup> (2.0-3.3)	10.6 <sup>  </sup> (4.7-21.9)	21.5 <sup>  </sup> (10.7-37.7)	48.3 <sup>§#</sup> (24.6-67.2)

\* Mean (range)

† DCR = dilated cardiomyopathy rabbit model

‡ Control vs. Group II,  $p < 0.05$ , statistically significant

§ Control vs. Group III,  $p < 0.05$ , statistically significant

<sup>||</sup> n = 4, <sup>||</sup> n = 3, <sup>#</sup> n = 5

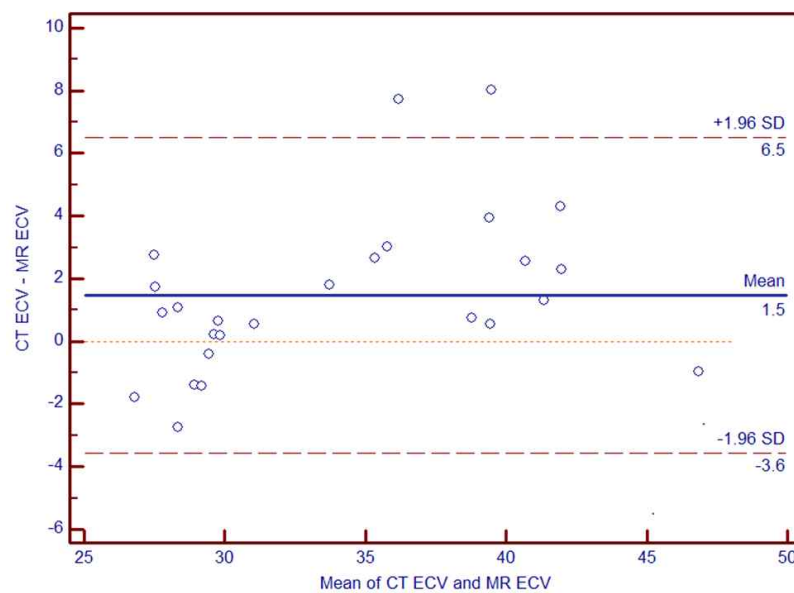


**Figure 9.** Bland-Altman Comparison of CT ECV and MR ECV



### **C. Comparison between CT, MR ECV and histologic collagen volume fraction**

CT ECV measured with dual-energy CT correlated with histologic CVF ( $n = 15$ ,  $r = 0.811$ ,  $p < 0.001$ ) and MR ECV correlated with histologic CVF ( $n = 15$ ,  $r = 0.946$ ,  $p < 0.001$ ). There was good correlation between CT ECV and MR ECV in all groups ( $n = 26$ ,  $r = 0.888$ ,  $p < 0.001$ ), and post-modeling groups ( $n = 11$ ,  $r = 0.840$ ,  $p < 0.001$  )

#### IV. DISCUSSION

The aims of this study were to validate ECV fraction using dual-energy CT and to compare it with contrast-enhanced MRI and histologic findings. We have demonstrated a DCR model for radiologic and histological evaluation of diffuse myocardial fibrosis. A previous study reported that after administration of doxorubicin at the dose of 1 mg/kg twice a week for only 6 weeks is safe and sufficient to induce dilated cardiomyopathy in rabbits with low mortality rate.<sup>19</sup> We followed the same methods to make DCR models. However, initially the mortality was unexpectedly high. Among the twelve rabbits, five rabbits were dead before 6 weeks. The reason was probably that quarantine equipment was not available. So we did nutritional supports with kale and cabbage every day and added intramuscular injection of antibiotics every day from 5 weeks after modeling. Recently, myocardial fibrosis imaging based on T1-mapping and ECV measurement is regarded as a promising tool to detect and quantify diffuse myocardial fibrosis, which can overcome the limitation of LGE imaging. The usefulness of T1 mapping MR imaging for quantification of diffuse myocardial fibrosis is demonstrated in various cardiac diseases.<sup>8,9,20-27</sup> Flett et al. reported a new MRI method using a concept of extracellular volume fraction to assess diffuse myocardial fibrosis using equilibrium contrast MRI.<sup>1</sup> ECV has been proven to be reliable and reproducible parameters with less MRI parameters influenced by other confounding factors such as scan timing, concentration of contrast, field strength, different vendor platforms, and patients' renal function status.<sup>2,28,29</sup>

However, MR has a few limitations such as motion correction, different scan position between pre- and post-contrast T1 mapping images, incomplete coverage of the heart, variable confounding factors affecting post-contrast T1 value.<sup>2,30,31</sup> etc. Most recently, Nacif et al.<sup>12,13</sup> reported the usefulness of measurement of myocardial ECV using bolus injected contrast

enhanced CT. They recruited 24 heart failure patients. ECVs of cardiac CT and MR were higher in patients than healthy controls. There was good correlation between ECV of cardiac CT and cardiac MR imaging ECV values ( $r = 0.82$ ,  $p < 0.001$ ). Of note, the radiation dose was not high ( $1.98 \text{ mSV} \pm 0.16$ ).<sup>12</sup> In another study, Bandula et al.<sup>11</sup> developed and validated equilibrium contrast-enhanced CT using continuous infusion after bolus injection protocol and compared with ECV from equilibrium contrast-enhanced magnetic resonance imaging and histologic reference. Equilibrium CT ECV was strongly correlated to equilibrium MR ECV ( $r = 0.73$ ) and also showed a significant correlation with histologic fibrosis ( $r = 0.84$ ,  $p < 0.001$ ). These studies showed the possibility of quantification of myocardial fibrosis using cardiac CT. CT has many advantages over MR; covering the whole myocardium in a short scanning time, low price, short scanning time, simultaneous evaluation of coronary arteries, etc. The previous study used conventional CT with both of pre-contrast and post-contrast equilibrium CT.<sup>11-13</sup> For the analysis, ROI of myocardial septum were selected on the post-contrast image and the matching pre-contrast image was selected by visual estimation. This method had misregistration errors due to changes in acquisition location of pre- and post-contrast CT. More importantly radiation exposure is doubled. We were cautioned by the difficulties of misregistration artifacts encountered when using conventional CT, as well as using the idea of visual estimation to match up the post-contrast image and the matching pre-contrast image. In our study we shifted the method to dual-energy CT which works with data acquired at the time of the scan to produce both images. Dual-energy CT would give data from CT imaging done at two different X-ray spectra at the same time.<sup>16</sup> The difference in material composition is shown because of different photon absorption rates being affected at the two spectra by the data.<sup>16,32</sup> The major advantages of dual-energy CT over conventional CT in this study are lack of misregistration errors occurring from pre- and

post-contrast scanings with different scanning time, different position. An iodine map reconstructed by data with simultaneous acquisition of 100 and 140 kVp contrast images through the one scan is sufficient to visualize myocardial perfusion, delayed contrast-enhancement dispense of two step pre- and post-contrast scanings. Our study is the first study assessing CT ECV using dual-energy CT. For validation of CT ECV values, we scanned repeatedly from 3 minutes to 20 minutes after the contrast injection. We demonstrated continuous CT ECV values without significant change. We used the 13 minute scan time image for the measurements for both CT ECV and MR ECV. We used the same equation as the previous CT ECV studies:  $(\Delta HU_m / \Delta HU_b) \times (1-Hct)$ , where  $\Delta HU = HU_{post} - HU_{pre}$ , which means the change of attenuation value (HU) between before and after administration of iodine contrast agents. On dual-energy CT measurement of HU of the ROI on the iodine map represents the degree of enhancement on the measured area. HU of the ROI on the iodine map is sufficient to measure  $\Delta HU$  of myocardium or blood cavity. Therefore, the equation was changed to  $(HU_m / HU_b) \times (1-Hct)$ , where  $HU_m = HU$  of ROI of myocardium on the iodine map,  $HU_b = HU$  of blood pool on the iodine map. We created a home-made software program that both measured the CT ECV and generated a color-coded iodine map which illustrated the distribution of iodine contrast in myocardium at a glance. The reported HU on the iodine map quantified the myocardial enhancement. This pilot study has laid out the steps necessary to conduct a broader examination of the dual energy CT, MRI, versus histology assessment of fibrotic cardiac disease. Although MRI has been the standard for imaging fibrosis the potential benefits of CT usage need to be recognized. CT can allow for fast, available, and economical imaging. This study shows the proof of concept using an animal model. Further studies are suggested for assessment in humans, which to our knowledge has not been pursued yet.

The limitations of our study include the small sample size, which

prevents the generalization of the data. The second limitation was estimation of exposed radiation dose was not available because repetitive scanings were done every two minute to validate scan protocol. And the image qualities of the iodine maps were not good because of the increased number of artifacts. 71 segments (28%) were score 2 (good) which can slightly affect diagnostic accuracy and 16 segments (6.3%) were nondiagnostic (score 1: poor). It was thought that the motion artifacts were caused by the rabbits' fast heart rate, and the low temporal resolution of dual energy CT. Although we used a drug to reduce heart rate, the mean heart rate of pre-modeling animal was  $114.3 \pm 29.5$  and that of post-modeling rabbit was  $98.2 \pm 17.3$ . However, this problem will be solved if applied to humans, because the human heart rate is lower in comparison to rabbits. Lastly, we correlated CT ECV with histologic CVF. Because there is no direct method to measure histologic ECV, we could not compare the relationship between CT ECV and histologic ECV. However, the correlation between the CT ECV and histologic CVF was statistically significant. Further studies are suggested for assessment in humans in a clinical setting to determine the quantification of the ECV using dual-energy CT with low radiation exposure.

## **V. CONCLUSION**

This study demonstrates that dual-energy CT is a noninvasive feasible method to measure diffuse myocardial fibrosis quantitatively using CT ECV without misregistration errors with lower radiation exposure. Although MRI has been the standard for imaging fibrosis the potential benefits of CT usage need to be recognized.

## VI. REFERENCES

1. Flett AS, Hayward MP, Ashworth MT, Hansen MS, Taylor AM, Elliott PM, et al. Equilibrium contrast cardiovascular magnetic resonance for the measurement of diffuse myocardial fibrosis: preliminary validation in humans. *Circulation* 2010;122:138-44.
2. Mewton N, Liu CY, Croisille P, Bluemke D, Lima JA. Assessment of myocardial fibrosis with cardiovascular magnetic resonance. *J Am Coll Cardiol* 2011;57:891-903.
3. Assomull RG, Prasad SK, Lyne J, Smith G, Burman ED, Khan M, et al. Cardiovascular magnetic resonance, fibrosis, and prognosis in dilated cardiomyopathy. *J Am Coll Cardiol* 2006;48:1977-85.
4. Kuruwilla S, Adenaw N, Katwal AB, Lipinski MJ, Kramer CM, Salerno M. Late gadolinium enhancement on cardiac magnetic resonance predicts adverse cardiovascular outcomes in nonischemic cardiomyopathy: a systematic review and meta-analysis. *Circ Cardiovasc Imaging* 2014;7:250-8.
5. Wu KC, Weiss RG, Thiemann DR, Kitagawa K, Schmidt A, Dalal D, et al. Late gadolinium enhancement by cardiovascular magnetic resonance heralds an adverse prognosis in nonischemic cardiomyopathy. *J Am Coll Cardiol* 2008;51:2414-21.
6. Bauner KU, Biffar A, Theisen D, Greiser A, Zech CJ, Nguyen ET, et al. Extracellular volume fractions in chronic myocardial infarction. *Invest Radiol* 2012;47:538-45.
7. Broberg CS, Chugh SS, Conklin C, Sahn DJ, Jerosch-Herold M. Quantification of diffuse myocardial fibrosis and its association with myocardial dysfunction in congenital heart disease. *Circ Cardiovasc Imaging* 2010;3:727-34.
8. Florian A, Ludwig A, Rosch S, Yildiz H, Sechtem U, Yilmaz A. Myocardial fibrosis imaging based on T1-mapping and extracellular volume fraction (ECV) measurement in muscular dystrophy patients: diagnostic

value compared with conventional late gadolinium enhancement (LGE) imaging. *Eur Heart J Cardiovasc Imaging* 2014;14:1004-12.

9. Thuny F, Lovric D, Schnell F, Bergerot C, Ernande L, Cottin V, et al. Quantification of Myocardial Extracellular Volume Fraction with Cardiac MR Imaging for Early Detection of Left Ventricle Involvement in Systemic Sclerosis. *Radiology* 2014;271:373-80.

10. Miller CA, Naish JH, Bishop P, Coutts G, Clark D, Zhao S, et al. Comprehensive validation of cardiovascular magnetic resonance techniques for the assessment of myocardial extracellular volume. *Circ Cardiovasc Imaging* 2013;6:373-83.

11. Bandula S, White SK, Flett AS, Lawrence D, Pugliese F, Ashworth MT, et al. Measurement of Myocardial Extracellular Volume Fraction by Using Equilibrium Contrast-enhanced CT: Validation against Histologic Findings. *Radiology* 2013;269:396-403.

12. Nacif MS, Kawel N, Lee JJ, Chen X, Yao J, Zavodni A, et al. Interstitial myocardial fibrosis assessed as extracellular volume fraction with low-radiation-dose cardiac CT. *Radiology* 2012;264:876-83.

13. Nacif MS, Liu Y, Yao J, Liu S, Sibley CT, Summers RM, et al. 3D left ventricular extracellular volume fraction by low-radiation dose cardiac CT: Assessment of interstitial myocardial fibrosis. *J Cardiovasc Comput Tomogr* 2013;7:51-7

14. McChesney EW, Hoppe JO. Studies of the tissue distribution and excretion of sodium diatrizoate in laboratory animals. *Am J Roentgenol Radium Ther Nucl Med* 1957;78:137-44.

15. Gerber BL, Belge B, Legros GJ, Lim P, Poncelet A, Pasquet A, et al. Characterization of acute and chronic myocardial infarcts by multidetector computed tomography: comparison with contrast-enhanced magnetic resonance. *Circulation* 2006;113:823-33.

16. Johnson TR, Krauss B, Sedlmair M, Grasruck M, Bruder H, Morhard D, et al. Material differentiation by dual energy CT: initial experience. *Eur*

Radiol 2007;17:1510-7.

17. Lalande A, Salve N, Comte A, Jaulent MC, Legrand L, Walker PM, et al. Left ventricular ejection fraction calculation from automatically selected and processed diastolic and systolic frames in short-axis cine-MRI. *J Cardiovasc Magn Reson* 2004;6:817-27.

18. Baldy C, Douek P, Croisille P, Magnin IE, Revel D, Amiel M. Automated myocardial edge detection from breath-hold cine-MR images: evaluation of left ventricular volumes and mass. *Magn Reson Imaging* 1994;12:589-98.

19. Gava FN, Zacche E, Ortiz EM, Champion T, Bandarra MB, Vasconcelos RO, et al. Doxorubicin induced dilated cardiomyopathy in a rabbit model: an update. *Res Vet Sci* 2013;94:115-21.

20. Banyersad SM, Sado DM, Flett AS, Gibbs SD, Pinney JH, Maestrini V, et al. Quantification of myocardial extracellular volume fraction in systemic AL amyloidosis: an equilibrium contrast cardiovascular magnetic resonance study. *Circ Cardiovasc Imaging* 2013;6:34-9.

21. Kozak MF, Redington A, Yoo SJ, Seed M, Greiser A, Grosse-Wortmann L. Diffuse myocardial fibrosis following tetralogy of Fallot repair: a T1 mapping cardiac magnetic resonance study. *Pediatr Radiol* 2014;44:403-9.

22. Lu M, Zhao S, Yin G, Jiang S, Zhao T, Chen X, et al. T1 mapping for detection of left ventricular myocardial fibrosis in hypertrophic cardiomyopathy: a preliminary study. *Eur J Radiol* 2013;82:e225-31.

23. Moon JC, Treibel TA, Schelbert EB. T1 mapping for diffuse myocardial fibrosis: a key biomarker in cardiac disease? *J Am Coll Cardiol* 2013;62:1288-9.

24. Neilan TG, Coelho-Filho OR, Shah RV, Feng JH, Pena-Herrera D, Mandry D, et al. Myocardial Extracellular Volume by Cardiac Magnetic Resonance Imaging in Patients Treated With Anthracycline-Based Chemotherapy. *Am J Cardiol* 2012;111:717-22.



25. Puntmann VO, Voigt T, Chen Z, Mayr M, Karim R, Rhode K, et al. Native T1 mapping in differentiation of normal myocardium from diffuse disease in hypertrophic and dilated cardiomyopathy. *JACC Cardiovasc Imaging* 2013;6:475-84.
26. Sado DM, Flett AS, Banyersad SM, White SK, Maestrini V, Quarta G, et al. Cardiovascular magnetic resonance measurement of myocardial extracellular volume in health and disease. *Heart* 2012;98:1436-41.
27. Tham EB, Haykowsky MJ, Chow K, Spavor M, Kaneko S, Khoo NS, et al. Diffuse myocardial fibrosis by T1-mapping in children with subclinical anthracycline cardiotoxicity: relationship to exercise capacity, cumulative dose and remodeling. *J Cardiovasc Magn Reson* 2013;15:48.
28. Jellis CL, Kwon DH. Myocardial T1 mapping: modalities and clinical applications. *Cardiovasc Diagn Ther* 2014;4:126-37.
29. Lee JJ, Liu S, Nacif MS, Ugander M, Han J, Kawel N, et al. Myocardial T1 and extracellular volume fraction mapping at 3 tesla. *J Cardiovasc Magn Reson* 2011;13:75.
30. Kellman P, Hansen MS. T1-mapping in the heart: accuracy and precision. *J Cardiovasc Magn Reson* 2014;16:2.
31. Gai N, Turkbey EB, Nazarian S, van der Geest RJ, Liu CY, Lima JA, et al. T1 mapping of the gadolinium-enhanced myocardium: adjustment for factors affecting interpatient comparison. *Magn Reson Med* 2011;65:1407-15.
32. Graser A, Johnson TR, Chandarana H, Macari M. Dual energy CT: preliminary observations and potential clinical applications in the abdomen. *Eur Radiol* 2009;19:13-23.

<ABSTRACT(IN KOREAN)>

확장성 심근병증 토끼에서 이중에너지 전산화 단층 촬영술을 이용한  
심근 세포 외 부피 측정: 자기공명영상을 이용한 심근 세포 외 부피 및  
조직학적인 소견과 비교

<지도교수: 최 병 옥>

연세대학교 대학원 의학과

홍 유 진

최근 개발된 자기공명영상의 T1 지도화 기법은 이전 지연 조영 증강 영상으로 영상화할 수 없는 미만성 심근 섬유화를 조기발견하고 정량화할 수 있는 유용한 기법으로 자리 잡고 있다. 전산화 단층 촬영술에서 이용하는 요오드 조영제가 자기공명영상에서 쓰이는 가돌리늄 조영제가 이 세포 외 부피 조영제이며 비슷한 동역학을 보인다는 이론에 근거하여 전산화 단층 촬영술로 세포 외 부피를 정량화할 수 있음이 증명되었다. 따라서 본 연구에서는 이중에너지 전산화 단층 촬영술을 이용하여 심근 세포 외 부피를 측정하고 이를 자기공명영상을 이용한 심근 세포 외 부피 값과 조직학적 섬유화 정도와 비교하고자 하였다.

토끼에 독소루비신을 일주일에 2번씩 1.0 mg/kg 용량으로 정맥 주입하여 심근 섬유화 모델을 제작하였으며 섬유화 모델을 만들기 전과 만든 후 6주, 12주 16주에 이중에너지 조영 증강 전산화 단층 촬영술과 자기공명영상 (조영 증강 T1 지도화 기법영상, 영화영상기법영상)을 시행하였다. 전산화 단층 촬영과 자기공명영상 촬영은 2시간 이내 시행하였다. 자기공명 영화영상을 이용하여 좌심실 기능을 측정하였으며 이중에너지 전산화 단층 촬영술을 이용하여 얻은 요오드 지도와 T1 지도화 기법 자기공명영상으로 얻은 조영 전, 후 T1 지도화 이미지를 이용하여 세포 외 부피를 측정하였다. 세포 외 부피는

심실 단축 면 영상 유두 근이 보이는 좌심실 중간 중격 부분에 관심영역을 그려 측정하였으며 전산화 단층촬영 이미지와 자기 공명 영상 이미지 상 최대한 동일한 부위에서 측정하였다.

총 15마리 토끼를 심근 섬유화 모델을 제작하기 전 전산화 단층 촬영술과 자기공명영상을 촬영하였으며 이중 4마리는 정상토끼의 조직학적 소견을 위해 희생하였다. 11마리의 심근 섬유화 모델을 제작하였으며 모델링 후 6주 ( $n = 11$ ), 12주 ( $n = 8$ ), 16주 ( $n = 5$ )에 추가로 영상을 얻었다. 조직학적인 소견을 위해 6주 촬영 직후 3마리, 12주 촬영 직후 3마리, 16주 촬영 직후 5마리를 희생하여 picrosirius red 염색 후 슬라이드를 제작하였다.

전산화 단층 촬영술을 이용한 요오드 지도에서 켄 세포 외 부피는 6주 모델(11마리), 12주 모델(8마리), 16주 모델(5마리)에서 각각 28.5% (25.9-31.3), 35.3% (30.2-40.1), 41.9% (35.6-44.1), 42.1% (39.2-46.4),  $p < 0.001$ )로 점점 증가하는 양상을 보였고 자기공명 영상에서 측정한 세포 외 부피와 높은 연관성을 보였으며 조직학적인 섬유화 정도와도 높은 연관성을 보였다.

본 연구를 통하여 이중에너지로 얻은 세포 외 부피가 자기공명영상으로 기법에서 얻은 세포 외 부피와 조직학적인 섬유화 정도와 높은 일치도를 보임을 증명하였으며 결론적으로 이중에너지 전산화 단층 촬영술은 한 번의 스캔으로 오등록 오류 없이 심근 섬유화를 정량화할 수 있는 비 침습적인 유용한 영상기법이다.

---

핵심되는 말 :자기공명 영상, 이중에너지 전산화 단층 촬영술, 심근 섬유화, 세포외 부피